Applied Geochemistry 26 (2011) 666–678

Contents lists available at ScienceDirect

Applied Geochemistry

journal homepage: www.elsevier.com/locate/apgeochem

Speleothems and pine trees as sensitive indicators of environmental pollution – A case study of the effect of uranium-ore mining in Hungary

Zoltan Siklosy [a,*], Zoltan Kern [a,1], Attila Demeny [a], Sebastian Pilet [b], Szabolcs Leel-Ossy [c], Ke Lin [d], Chuan-Chou Shen [d], Eva Szeles [e], Daniel Breitner [f]

[a] Institute for Geochemical Research, Hungarian Academy of Sciences, Budapest, Hungary
[b] Institute of Mineralogy and Geochemistry, University of Lausanne, Switzerland
[c] Eotvos University, Budapest, Hungary
[d] High-precision Mass Spectrometry and Environment Change Laboratory, Department of Geosciences, National Taiwan University, Taipei, Taiwan, ROC
[e] Institute of Isotopes, Hungarian Academy of Sciences, Budapest, Hungary
[f] Atomic Energy Research Institute, Hungarian Academy of Sciences, Budapest, Hungary

ARTICLE INFO

Article history:
Received 12 August 2009
Accepted 5 January 2011
Available online 9 January 2011
Editorial handing by R. Fuge

ABSTRACT

Four decades of U ore production in Hungary provides an opportunity to study the possible environmental effects of mining. The study reveals significant changes in chemical composition of a stalagmite (cave deposit). The good fit between U content changes in the studied deposit and the U ore production rate support the assumption of the relationship with mining activity. An independent chemoenviromental archive, living pine (Pinus sylvestis) trees were also investigated. Data on pine tree cores collected from the same region show different levels of pollution (Cu, Zn, Mn, U) after the 1950s and 1960s, linked to the opening of mines and subsequent dust fallout around the site. Elevated concentrations of detritally derived elements (Si, Al, Th) coupled with a rise in U concentration and change in $\delta^{234}U$ values of the stalagmite suggest increasing amounts of mine-derived dust from 1 to 3 km distance that settled and washed into the karst system. The combined usage of different proxies not only provides historic records for the anthropogenic impact in the environment, but also allows the timing of U concentration increases within the stalagmite and the identification of elemental behavior from the pollution. This study shows that complementary geochemical archives such as stalagmites and tree rings used together can enhance understanding of past environmental contamination.

1. Introduction

Environmental pollution can be indirectly monitored by investigating the biosphere, i.e. living organisms (Panov et al., 1999; Bellis et al., 2001; Ferretti et al., 2002; Thiry et al., 2005; Dunca et al., 2005; Saunders et al., 2007), or geological material such as lake sediments (O'Sullivan, 1983; Whitlock et al., 2008), and coastal and river deposits (Perin et al., 1997; Cooksey and Hyland, 2007). The traces of historical anthropogenic activities can also be detected at sites of large scale pollution (e.g. Schettler and Romer, 2006; Costagliola et al., 2008). However, continuously depositing geological formations, i.e. speleothems (cave deposits) have significant advantages over other natural archives. Stalagmites develop in relatively protected environments, practically free from redeposition and alteration, they are widespread in continental karstic areas and they can be dated by absolute radiometric methods (Richard and Dorale, 2003; Fairchild et al., 2006).

Speleothems or cave calcites are formed when water saturated in CO_2 from the soil zone enters a cave and the CO_2 degasses (Hill and Forti, 1997). These deposits are ideal as multi-proxy continental archives with the potential to provide information about changes in precipitation and temperature that has played a role in human history. Cave deposits of well selected sites reflect global climate signals and environmental changes (e.g. Spötl et al., 2002; Wang et al., 2006), although their potential for monitoring environmental pollution has not yet been fully explored (Borsato et al., 2007; Perrette et al., 2008). The globally increasing anthropogenic emission of S into the atmosphere has been recorded by investigation of stalagmites using XANES techniques (Frisia et al., 2005) or confirmed independently (Fairchild et al., 2009). Volcanism may serve as a natural analogue of environmental pollution and speleothems may capture evidence for past volcanic eruptions (Baker et al., 1995; Frisia et al., 2005; Siklosy et al., 2007, 2009), but the investigation of short-term pollution events requires high-resolution chemical analyses of the speleothems.

* Corresponding author. Fax: +36 1 319 3137.
E-mail address: siklosy@geochem.hu (Z. Siklosy).
[1] Present address: Department of Paleontology, Eötvös University, Budapest, Hungary.

0883-2927/$ - see front matter © 2011 Elsevier Ltd. All rights reserved.
doi:10.1016/j.apgeochem.2011.01.025

As a further application of stalagmite research in environmental monitoring, the current study describes the effects of a major contamination source (i.e. U mining) in south-Hungary using high-resolution analytical techniques. Uranium concentrations in stalagmites are typically much less than 1 ppm. The incorporation of U in calcite provides the basis for U-series age-dating methods (i.e. Richard and Dorale, 2003), which have proven to be valuable geochronological tools for studies of both marine and terrestrial carbonates.

Uranium is readily mobilized in the meteoric environment, principally as the highly soluble uranyl ion (UO_2^{2+}) and its complexes, the most important of which are the stable carbonate complexes that form in typical groundwaters (pH > 5; Gascoyne, 1992). Considering the mobilility of U^{6+} (uranyl ion) in an oxidizing environment, the major part of the polluting U would not be expected to accumulate in soils, as was found by Kratz and Schnug (2005); rather, the U (e.g. applied with P fertilizers) is expected to be transported in groundwater.

The presence and mobility of the dissolved U within the aqueous karst system, therefore, is directly influenced by fall-out dust deposited at the surface without further restriction or adsorption. Soil- column experiments have shown that humic acid influences the transport of both U(IV) and U(VI). In the presence of humic acids both redox species migrate nearly as fast as the groundwater flow. In the case of U(VI) humic acid exhibits a clear mobilizing effect (Sachs et al., 2005). Uranium (VI) mobility in soils may be limited by the formation of low solubility complexes, and by adsorption, preferably to Fe and Mn oxyhydroxides, organic matter and clays (Langmuir, 1978; Ribera et al., 1996). The coarse textured, low organic-matter soil described at the site has a low clay content. Moreover in solutions of circumneutral pH, the presence of carbonate ions (karstic area) induces the formation of stable uranyl-carbonate complexes (Finch and Murakami 1999). These highly soluble complexes are mainly neutral or negatively charged, minimizing adsorption to soil particles and enhancing U mobility (Elless and Lee, 1998; Finch and Murakami, 1999).

Uranium-ore mining in Hungary occurred exclusively in the area described in this study. The (deep) pit mine produced about 500 t of U concentrate annually during its operation (1957–1997) and million of tons of solid material were excavated with possible effects on the surrounding environment. To follow the depositional history of contamination and its possible relationship with recent carbonate formations and local plants during the past hundreds years, analyses of cave deposits (speleothems) and living pine trees were carried out.

Preliminary studies reported elevated U concentrations on dried and milled tree leaves within the vicinity of one of the ventilation-shafts of the U mine (Bozsó, 1999). It was concluded that the emitted radiogenic dust could settle some hundreds of meters away from the ventilation funnel with high concentrations being controlled by topographic features and vegetation cover. Thus, the existence and the transport of the pollution were assumed, however the extent of the affected region is still unknown. For this study it was assumed that the fall-out material and its chemical composition could also modify the composition of seepage water and, therefore, the geochemistry of the speleothems actively forming from dripping waters.

The objective of this study was to determine the possible effect of the 4-decade-long U mining on the environment by the investigation of a stalagmite from the nearest cave in the region. The aim was to detect the possible traces of the assumed pollution by analysing a stalagmite as a continuously precipitating formation covering the last 100 a. As a complementary study two pine trees were also analysed. Here, with the applied high-resolution techniques the role of the U mine on polluting the wider catchment area of the cave can be verified.

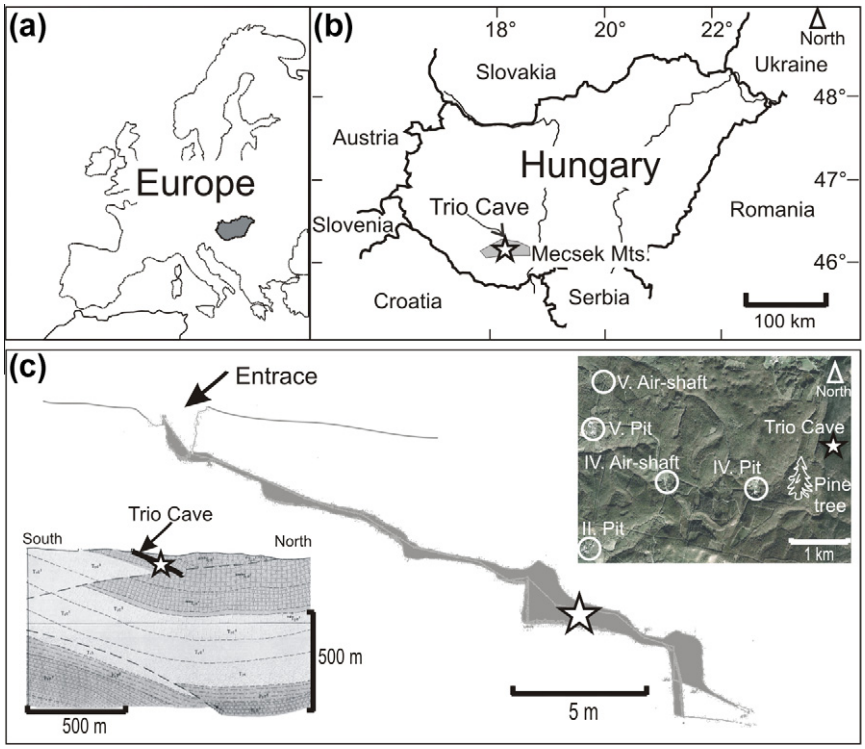

Fig. 1. (a) Location of Hungary in Europe; (b) location of Trio Cave in Southern Hungary; (c) schematic cross-section of the Trio Cave and the surroundings with the sample location, indicated by cross (courtesy of the SZKBE cave explorer group in 2001–2002). U-ore mining pits and ventilation shafts are also indicated on the aerial photograph (courtesy of Mecsekérc Ltd.). Latin numbers are used to label ventilation shafts and mine-pits, following the nomenclature of the mining company.

2. Site description

2.1. Physical and geological setting of the Trio Cave

The Trio Cave (46.7°N, 18.9°E) is located in the western part of the Mecsek Mts, S-Hungary (Fig. 1a) at the bottom of the Szuado Valley, approx. 1.5 km east of the nearest entrance and the ventilation-shaft of the U mine (No. IV mine-pit) and 12 km NW of a power plant that was coal-fired before 2003. The cave is one of the karst systems developed in anisian Lapis Limestone in the area and contains ca. 200 m of passages with a catchment area of 3.5 km^2. There is only one artificially expanded entrance opened in 1969, but soon after was flooded and became inaccessible due to insufficient flood protection. In 1997 the problem was finally solved and the cave opened for speleologists. The cave is situated in a natural oak and hornbeam forest free from agricultural activities (i.e. ploughing, etc.).

The geology of the region has been extensively studied due to U ore exploration and the interest in mining the area (Fig. 1b). Uranium mining in Hungary was based on deposits discovered in the southern part of the country, in the vicinity of the city of Pécs, in thick (>1000 m) Upper Permian fluviatile sandstones of the Western Mecsek Mts (Fazekas, 1987; Bleahu et al., 1996; Barabás and Barabás-Stuhl, 2005). These rocks were followed by Triassic shallow marine clastics and carbonates (limestones and dolomites with evaporites interbedded; Nagy, 1968).

The mean annual temperature within the interior of the cave is ca. 9.8 °C, the average precipitation in the region is ca. 660 mm/a (see Supplementary material for details). The general direction of the wind is westerly to north-westerly.

2.2. Uranium mining activity

Five mine pits were excavated during the industrial scale U ore production from 1954, covering ca. 65 km^2 (Nos.: I–V, according to the nomenclature of the mine). During the 1980s the predominant part of the mine production penetrated deeper and deeper levels in the Permian sandstone, increasing the cost of production. This, and world market U price lead to economically unfavorable conditions and a decision was made to close all of the U mines in 1997. The U production and the amount of the excavated host rock from the pits were precisely recorded, thus the most productive and declining periods are known (Fig. 2). Host rocks with 125–130 ppm U were mined and removed. Pit No. II (ca. 3 km away from the catchment of the Trio Cave) was opened in 1954 and reached its maximum activity at the end of the 1960s, with a general decrease in production afterwards. Pit No. IV, the one closest the Trio Cave (ca. 1 km), was opened in 1965, and after a rapid increase a plateau-like maximum was produced, and the annual production started to decrease by the end of the 1980s The youngest pit (No. V) was opened in 1975 and reached its maximum at the end of the 1980s.

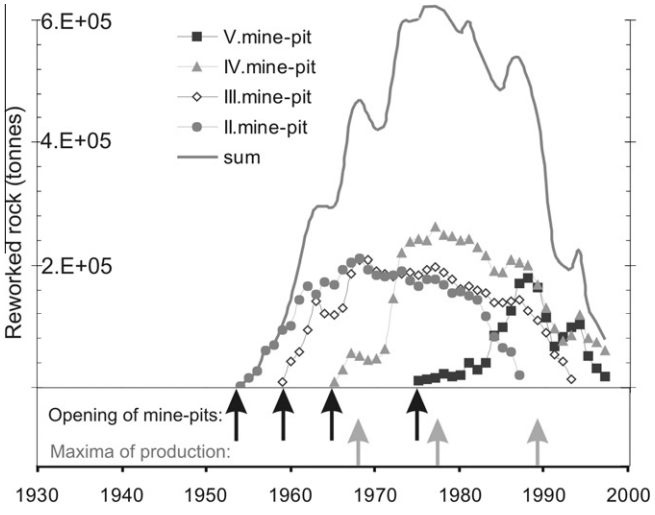

Fig. 2. History of U ore production, as shown by the mass of reworked U-bearing sandstone (courtesy of Mecsekérc Ltd., unpublished reports) in calendar years (AD). The date of the opening of the different mine-pits (black arrows) and their maximum productions (grey arrows) are also indicated.

3. Sampling and analytical methodology

3.1. Sampling

3.1.1. Stalagmite

In order to follow environmental changes over the last ca. 50 a an actively growing stalagmite (named "beehive oven" based on its morphology; see Fig. 3b) was sampled with a core-driller in 2001. The drilled sample revealed the internal structure of the dome-like stalagmite, with bent laminae representating its core and parallel laminae along its rim (Fig. 3a and b). The 42 cm long (partly broken) drilled sample is composed of white to brownish, partly laminated calcite. For this study the sub-recent part of the core was selected with a total length of 27 mm from the actively growing surface. The core was cut in half with a speed controlled diamond saw parallel to its growth direction. One half had been stored and the other was diamond-paste polished, and cleaned in distilled water in an ultrasonic bath. A thin slice from the polished sample was separated for laser-ablation ICP-MS studies, while the remaining material was used for stable isotope investigation and age determinations. The youngest 27 mm piece of the drill core was selected for this study as it should represent the last several hundred years.

3.1.2. Pine tree

Two healthy Scots pine (*Pinus sylvestris* L.) trees were selected for dendrochemical investigation (Table 1). They grow on the small ridge (46.11 N, 18.15 E, 395 m asl) located between the U-mine shafts and Szuadó Valley at the western border of the watershed of Trio Cave (Fig. 1b). Despite the fact that pine is not an indigenous species in the area, this exotic conifer was selected for the study as evergreen species are thought to be more sensitive to changes in atmospheric chemistry than deciduous trees due to their larger leaf area/volume ratio and permanency of foliage (Cutter and Guyette, 1993). Trees with pathogen activity or mechanical damage on their surface were avoided (Smith and Shortle, 1996).

Two cores were extracted from the bole by increment borer on 8 December, 2008 during the period of winter dormancy to test for changes in dendrochemical signals due to potential seasonal variations in trace element concentrations (Hagemeyer and Schäfer, 1995).

One core was used for the local pine chronology the other was retained for chemical analysis. A part of the bark was peeled by a stainless steel knife to remove surface contamination of the wood by accumulated airborne dust on the bark surface (Schulz et al., 1999). Samples were packed in plastic straws and stored frozen at ca. −10 °C until analysis to prevent fungal growth (Smith and Shortle, 1996) and sap migration (Pearson et al., 2006).

Two functionally different parts can be distinguished in the stem of woody plants. The outer part, called sapwood, contains the living cells while the inner part, called heartwood, has ceased to contain living cells (Kaennel and Schweingruber, 1995). The heartwood/sapwood boundary (H/S) was recorded in each core due to its important physiological divisional role (Smith and Shor-

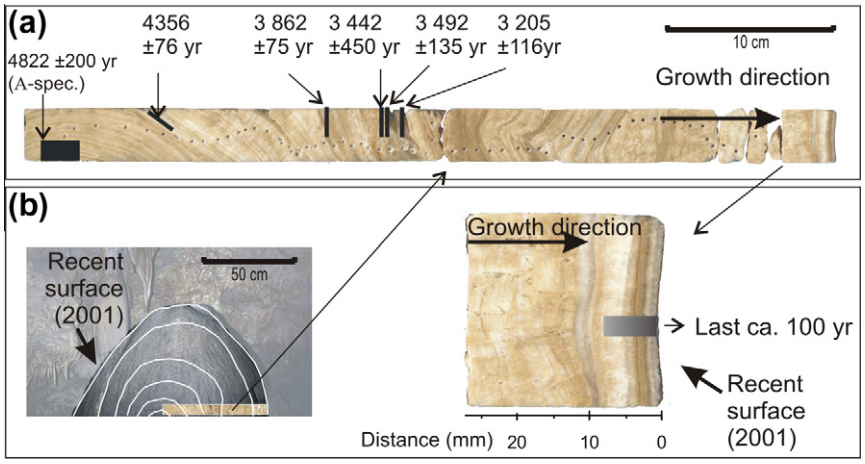

Fig. 3. (a) Image of the drilled stalagmite core. Positions of the U–Th age data reported are indicated by black vertical bars. (b) Image of the Trio stalagmite, called "beehive oven" and the position of the drilled core. White lines represents the morphological features. On the right the sub-recent part of the stalagmite core is shown, and covers approximately 100 a.

Table 1
Basic information about the dendrochemically investigated tree (OR: oldest sampled ring, OC: oldest chemically analysed ring, H/S: sapwood and heartwood boundary, MR: mean ring width).

Tree rings			H/S	MR (±stdev) (mm)	Distance (m) from the pit/ air shaft		
Code	OR	OC			II	IV	V
Kov06	1901	1939	1954	1.44 ± 0.67	4300/ 3200	780/ 2550	4150/ 4500
Kov09	1898	1929	1944	1.83 ± 1.51	4300/ 3200	780/ 2550	4150/ 4500

tle, 1996). The boundary was identified by visual inspection after thawing, when the sap was still moist; and also by the colour difference between sapwood and heartwood in dried samples. Nine additional pine trees were sampled to develop a local tree ring width chronology against which the chemically analysed cores could be checked.

Growth/climate analysis revealed that pine growth is dominated by May–June-July precipitation ($r = 0.56$, $p < 0.001$), and February–March mean temperatures act as a secondary growth regulator ($r = 0.30$, $p < 0.01$). Details on methods and results of growth/climate analysis are briefly presented in Supplementary material.

3.2. Analytical methods

3.2.1. Dating

An initial attempt was made to date the selected section of the stalagmite with U/Th but was unsuccessful due to (i) a high detrital contamination component and (ii) the small amount of ^{230}Th produced by U decay. Therefore, an age estimation was made on the basis of general growth rates determined for the older part of the stalagmite (see Supplementary material and Siklosy et al., 2009).

3.2.2. U–Th isotopic measurements

Five subsamples of the stalagmite (0.1–0.2 g; Fig. 4a) were drilled to obtain samples for U–Th chemistry (Shen et al., 2003) and ^{230}Th-dated isotopic measurements on a multi-collector-inductively coupled plasma mass spectrometer (MC-ICP-MS), Thermo Electron Neptune in the High-precision Mass Spectrometry and Environment Change Laboratory (HISPEC, Frohlich et al., 2009; Shen et al., 2010), Department of Geosciences, National Taiwan University. A triple-spike, ^{229}Th–^{233}U–^{236}U, isotope dilution method was employed to correct mass bias and determine U concentration (Shen et al., 2002). A protocol, using one newly-developed MasCom secondary electron multiplier with repelling potential quadrupole, was employed (Shen et al., 2010). Only 1–4 ng of U is required to obtain the 2-sigma reproducibility of 1–2‰. No significant difference between measurements of standards and carbonate samples on ICP-sector-field-MS (Shen et al., 2002) and on MC-ICP-MS certify the developed MC-ICP-MS methodology.

3.2.3. Chemical composition

Trace element compositions were determined by a laser-ablation-ICP-MS technique, parallel to the growth axes. Technical details are presented in Table 2. Data were reduced using the CONVERT and LAMTRACE programs. The error is estimated to lie between 5% and 10% on a relative basis (Günther et al., 1997).

For this study there was a critical need to establish a trace element proxy for the section representing the natural variability, hence the total length of the most recent part of the stalagmite (27 mm from the actively growing surface) was selected for high-resolution analyses.

3.2.4. Micro-XRF and micro-XANES analysis

In order to provide information on the microscopic heterogeneity and the chemical form of U present in the sample additional methods were selected. Synchrotron based X-ray analytical methods (micro-XRF and XANES) were used for determining the valence state of U in the stalagmite at the micro-fluorescence Beamline L of HASYLAB (Hamburg, Germany). The white beam of a bending magnet was monochromatized by a Si(1 1 1) double monochromator. A polycapillary half-lens (X-ray Optical Systems) was employed for focusing a beam of 1×1 mm^2 down to a spot size of 15 μm diameter. The absorption spectra were recorded in fluorescent mode, tuning the excitation energy near the L3 absorption edge of U by stepping the Si(1 1 1) monochromator, while recording the U-Lα fluorescent yield using an energy-dispersive Radiant silicon drift detector. The energy step size varied between 0.5 (edge region) and 2 eV (more than 50 eV above the edge), UO_2, UO_3 and U_3O_8 particles were used as standards. The collection of the elemental maps was performed at an excitation energy of 17.5 keV.

3.2.5. Dendrochemical analysis

The increment core was sectioned into 3 cm long subsamples and their surfaces were trimmed, perpendicular to fibres using a

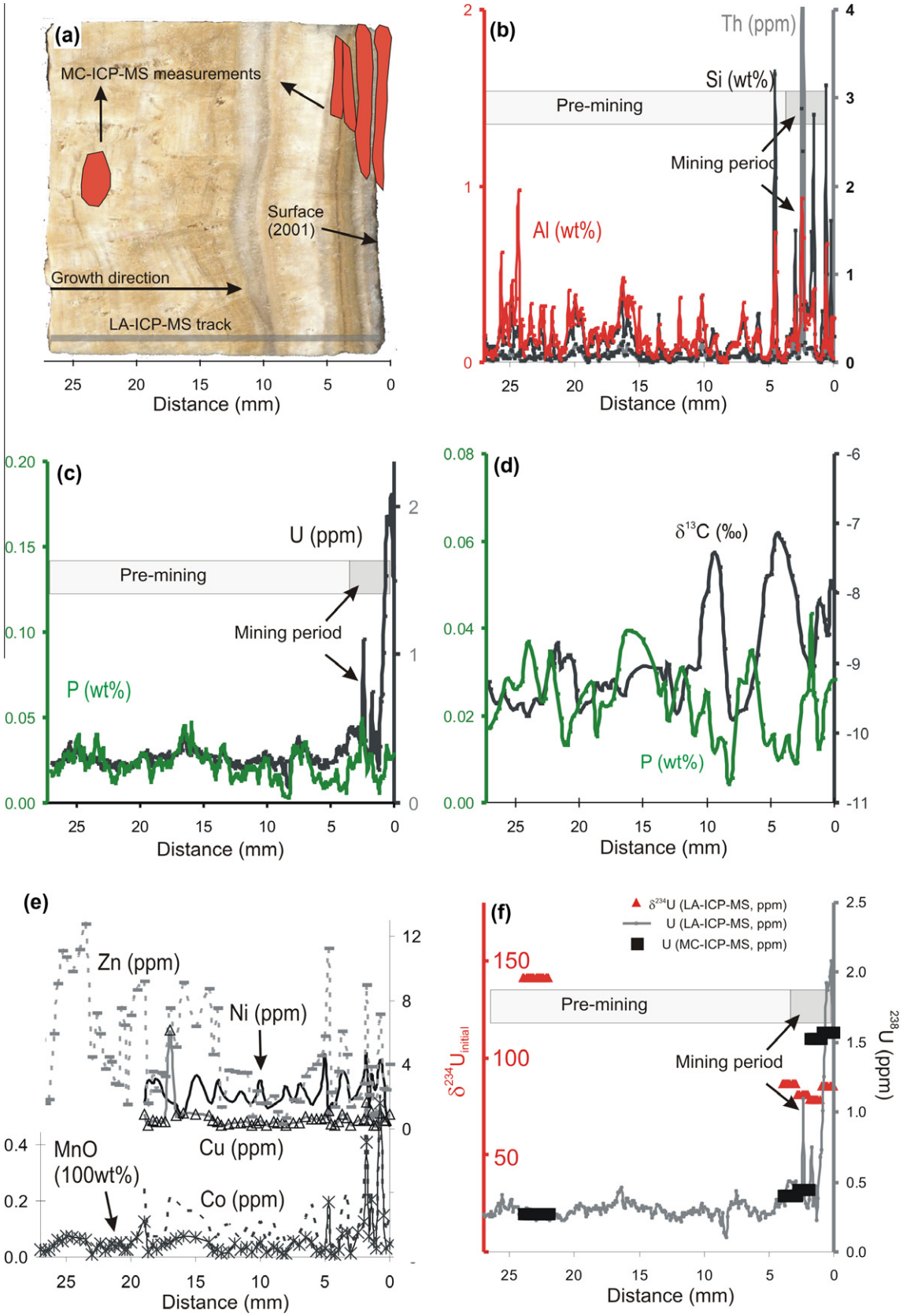

Fig. 4. (a) Image of the sub-recent part of Trio stalagmite core. Grey bar at the bottom shows the position of the trace-element profile. Position of the Multi Collector-Inductively Coupled Plasma-Mass Spectrometry (MC-ICP-MS) data is indicated by the dark grey regions; (b) Th, Al and SiO_2 contents; (c) P vs. U contents; (d) stable C isotope and P concentrations of the stalagmite; (e) Zn, Ni, Cu, Mn and Co contents; (f) U (^{238}U) concentration (measured independently by Laser Ablation- and MC-ICP-MS) and $\delta^{234}U$ values of the Trio stalagmite. All data are plotted against the distance from the active surface of the stalagmite (time of collection: 2001).

Table 2
Summary of the applied analytical techniques on the speleothem and wood samples.

	Stalagmite sample analysis	Dendrochemical analysis
Instrument	LA-ICP-MS	LA-ICP-MS
Host	University of Lausanne, Switzerland	Institute of Isotopes, Hungarian Academy of Sciences
Type	Perkin-Elmer ELAN 6100 DRC	Element2 ICP-MS, Thermo
Laser-type	LAMBDA PHYSICS	UP-213, New Wave Inc
Settings	7 Hz, 28 kV, energy ~170 mJ, fluency ~13 J/cm^2	10 Hz, 70%: 0.244 mJ
Spot size	60 μm	95 mm,
Standards	NIST612, BCR-2 glass	NIST 612
Normalized	Microprobe measurements of Ca	^{13}C intensity
Error	5–10%	10%
Background for correction	~30s	60s

Teflon coated razor blade. The razor blade was rinsed in 5% v/w HNO_3 and distilled water between each subsample.

Radial trace-element profiles were determined by a laser-ablation-ICP-MS technique. Technical details are presented in Table 2. For the measurements, a line scan perpendicular to the tree rings was used applying a very low scan speed (50 μm s^{-1}) in order to improve the resolution of the elemental distribution. Prior to the measurement the surface of the tree core sample was removed (preablated) using a wide (300 μm) laser beam to remove the outer, possibly contaminated layer (Sheppard and Witten, 2005).

Measured intensity values were corrected for the background signal. As the elements of interest were present at variable concentrations within the wood samples, this approach ensures that no cross-contamination occurred between the samples. Each measured value was normalized by the corresponding ^{13}C intensity in order to correct for the possible different ablation efficiencies and wood density properties (Barrelet et al., 2006). The advantage of ^{13}C for internal standardization is that its signal intensity in the mass spectrum has the same order of magnitude as the signal intensities of the investigated isotopes (Prohaska et al., 1998). These relative intensity (RI) data not only allow comparison between differences in concentration between tree rings (Pearson et al., 2005) but also the differences in relative intensities are linearly related to concentration differences (Hoffmann et al., 1994).

Measured data related to the same tree ring were pooled for each element and the average values were correlated with the calendar date of each tree ring.

Eighteen elements were measured but only Mn, Zn, Cu and U will be discussed here as the latter three were found to resist radial mobility in a recent similar study (Monticelli et al., 2009) and Mn has also been proved to be useful for dendrochemical research (i.e. Guyette et al. 1992).

To test the intra-tree stability of the dendrochemical signal replicate measurements were established on Kov09. The replicates produced consistent results (see Supplementary material for details).

3.2.6. Standardization of dendrochemical data

The necessity of standardization of dendrochemical data before meaningful comparisons between trees can be made has long been recognized (Guyette et al., 1991; Hantemirov, 1992). Here a two-stage standardization procedure was adopted from Kern et al. (2009) following the idea of Hantemirov (1992) to treat heartwood and sapwood separately. First, heartwood values were ratioed to the mean of the longest common overlapping period covered by both heartwood sections, namely 1939–1944. Second, data related to sapwood rings were standardized. To do so element-specific radial trends (i.e. declining or increasing from the H/S transition toward to bark, Watmough, 1999) were modelled for both trees and for each studied chemical species by linear regression fit to the data of sapwood rings. The outermost ring was disregarded due to frequently observed anomalous values originating from the attached cambium (*e.g.* Fritz, 2007). Relative intensity values for the sapwood rings were divided by the corresponding values derived by the linear model. In the final step separately standardized sections were spliced.

This standardization method was applied for Mn, Zn and Cu. The U record was not standardized because the "natural" radial distribution profile is not simply linear (Thiry et al. 2005). The most characteristic feature is a relatively large concentration peak at the sapwood side of the H/S transition. Both studied pine trees showed this physiological U-peak and it is not possible to model and remove it using a linear trend. Hence, it was decided to leave the U records as relative intensities (Fig. 5).

For the sake of simplicity and comparison to the speleothem record results for the post-2001 rings are not discussed in the present study.

3.2.7. Ring width measurement

A LINTAB digital positioning table and TSAP Win 0.55 software (Rinn, 2005) were used for measuring the annual ring widths with a precision of 0.01 mm, as well as for crossdating the growth series by graphical comparison against the local Scots pine master chronology built from 11 trees. The results were checked for missing rings and dating error using the COFECHA software (Holmes, 1983).

Owing to the annual resolution and precise dating (Baillie, 1995), guaranteed by the crossdating procedure (i.e., Stokes and Smiley, 1968), changes in the trace element record detected in the wood could be definitely linked to particular tree ring(s) and to corresponding calendar years.

3.2.8. Stable isotope compositions of stalagmite

Carbon isotope compositions of drilled calcite samples at a spatial resolution of ~0.3 mm were determined using an automated carbonate preparation device (Gasbench II) and a Thermo Finnigan delta plus XP continuous flow mass spectrometer at the Institute for Geochemical Research (McCrea, 1950; Spötl and Vennemann, 2003). A total of 75 C isotope measurements were obtained from the drilled core. Standardization was conducted using laboratory calcite standards calibrated against the NBS-19 standard. The results are expressed in the δ-notation [$\delta = (R1/R2-1) \times 1000$] where R1 is the $^{13}C/^{12}C$ ratio in the sample and R2 the corresponding ratio of the standard (V-PDB), expressed in ‰. Reproducibilities for C isotope analyses are better than ±0.15‰.

4. Results

4.1. Age model

The ca. 42 cm long drilled stalagmite core from the Trio Cave grew from ca. 4.82 ka Before Present until 2001 (when the stalgmite core was collected). No directly measured age results exist for the youngest part of the stalagmite, because of its extremely low ^{230}Th content, reflecting the relatively low U content, high amount of detritals and it's young age.

Using the determined ranges for the growth rate, based on U–Th age data for the older part of the stalagmite (see Supplementary material for details), an approximate length representing 100 a was marked and studied on the sub-recent part of the stalagmite (Fig. 3b).

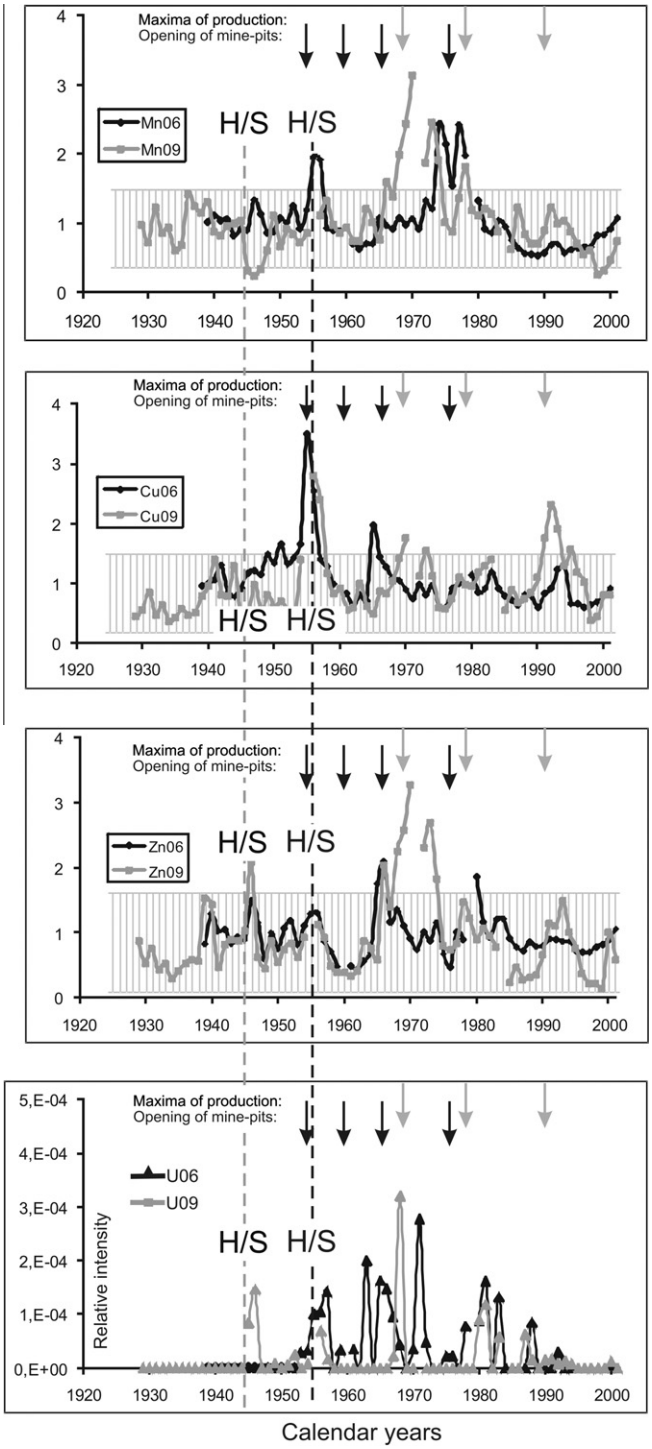

Fig. 5. Detrended Mn, Zn, Cu, indices and U relative intensities of the studied pine trees between 1929 and 2001 AD. The heartwood/sapwood boundaries (H/S, indicated) were recorded at 1954 and 1944 for Kov6 and Kov9, respectively. The date of the openings of the different mine-pits (black arrows) and their maxiumum productions (grey arrows) are also indicated, based on Fig. 2.

4.2. Trace-element profiles and stable carbon isotope compositions

The trace-element profile obtained from 251 single measurements along the studied section resulted in an averaged spatial resolution of approx. 107 μm. Both the trace element and stable C isotope record from the stalagmite are shown against distance (Fig. 4b–f), from the oldest part (27.1 mm) to the youngest (0 mm). Direct comparison with the stable isotope data using statistical analysis requires equidistant resolution for both datasets, thus the high-resolution trace-element profile was averaged to fit the less frequently drilled stable isotope data by taking the sizes and positions of the drilled and ablated pits into account. This method finally produced 75 trace element data points (Table 3) that were used for combined statistical analyses together with the $\delta^{13}C$ data.

Here three groups of elements are shown on the basis of their common behavior and origin, to clearly distinguish natural and anthropogenic processes. The first group of elements represents different *detrital* particles (Si, Al, Th), the second group are potentially powerful tracers of *biogenic* activity in the soil zone above the cave (P, $\delta^{13}C$ and U), while the third group represent *metals* which could have been recently introduced through human activity (Ni, Zn, Co, Cu and Mn).

Increased incorporation of debris derived from erosion of local rock formations can significantly affect the trace element composition of stalagmites (Fairchild et al., 2006). The presence of detrital impurities (i.e. clay minerals), in general, can be followed by the concentration of e.g. Si, Al and Th (Fairchild et al., 2006). The studied stalagmite section generally shows <0.5 wt.% Si and Al, and <0.15 ppm Th, although four spikes for Si (at 4.53–4.32, 2.48–2.27, 1.73–1.40 and 0.54–0.43 mm) and two large peaks for Th (at 2.38–2.27 and 0.54 mm) indicate the presence of major silicate-bearing impurities, all occuring between 4.7 and 0 mm (Fig. 4b). The youngest 3.3 mm in particular, is characterized by high Si, Al and Th contents. The elevated detrital content of the stalagmite can also be observed by its colour changes (Fig. 4a).

Phosphorus and U were plotted together, since these elements are directly linked to *vegetation* productivity and decay (Treble et al., 2003), i.e. leaching of organics from the soil (Johnson et al., 2006). Phosphorus and U are positively correlated with each other in most of the studied section, however, an abrupt U concentration increase was detected in the youngest part (starting at ca. 5 mm and especially between 1.3 and 0 mm), parallel with an increased detrital input. From a background value of 0.2–0.3 ppm, U increases gradually to about 2 ppm, followed by constant values for about 0.5 mm, and then its concentration decreases to about 1.5 ppm at the stalagmite's surface. Abrupt peaks are generally missing in the section, showing only low-amplitude cyclic variation (Fig. 4c).

The $\delta^{13}C$ values are plotted against distance in Fig. 4d and vary between −9.8 and −7.1‰. The isotope profile consists of 75 samples obtained at ca. 0.36 mm increments. Large positive shifts of 1.5 and 2‰ appear at or close to two distinct, translucent parts of the stalagmite section (at ca. 10 and 5 mm).

The concentration of the metals Ni, Co, Cu, Zn are plotted (Fig. 4e) to test the possible influence from a coal-fired power plant, 12 km SE of the study site. Zinc and Mn were measured over 27 mm sections; Ni, Co and Cu were determined between 19.5 and 0 mm. All the studied elements are above the detection limit. Zinc has higher concentrations at the beginning of the section, between 26 and 14 mm, with a maximum around 24–26 mm (above 15 ppm) compared to younger parts. Higher Cu, Ni and Co concentrations between 17.5 and 15 mm coincide with elevated P contents, but for the rest of the section the concentrations remain low, or become lower for these elements. Some of the peaks coincide with Si, Al and Th peaks. Manganese exhibits notable peaks (Fig. 4e) between 0–5 mm, and especially around 1–2 mm.

4.3. U isotope values

Uranium concentrations measured independently by MC-ICP-MS reproduced the U contents determined by the LA-ICP-MS technique, although the difference in spatial resolution resulted in a U

Table 3
Stable carbon isotope composition of stalagmite carbonate using a Thermo Finnigan delta plus XP mass spectrometer and trace element contents (in wt.% or ppm) determined by laser ablation ICP-MS analyses. Distance is measured from the very recent part of the stalagmite.

Distance (mm)	$d^{13}C$ V-PDB	Al_2O_3 (wt.%)	MgO (wt.%)	SiO2 (wt.%)	P_2O_5 (wt.%)	MnO * 100 (wt.%)	Co (ppm)	Ni (ppm)	Cu (ppm)	Zn (ppm)	Th (ppm)	U (ppm)
27.10	−9.26	0.11	0.06	0.27	0.02	0.03				7.00	0.04	0.26
27.00	−9.37	0.06	0.06	0.20	0.02	0.03				5.54	0.03	0.26
26.67	−9.57	0.04	0.06	0.14	0.02	0.02				1.59	0.02	0.27
26.33	−9.59	0.05	0.06	0.16	0.02	0.03				1.83	0.03	0.26
26.00	−9.43	0.12	0.06	0.21	0.03	0.04				5.92	0.06	0.32
25.67	−9.53	0.36	0.07	0.36	0.03	0.06				9.02	0.10	0.31
25.33	−9.65	0.31	0.06	0.32	0.03	0.06				11.10	0.08	0.35
25.00	−9.65	0.25	0.06	0.26	0.03	0.07				10.74	0.07	0.33
24.50	−9.58	0.24	0.06	0.26	0.03	0.07				9.79	0.08	0.32
24.00	−9.77	0.33	0.07	0.39	0.04	0.07				11.20	0.13	0.35
23.50	−9.51	0.67	0.06	0.35	0.03	0.06				12.78	0.09	0.32
23.00	−9.58	0.12	0.05	0.09	0.02	0.01				4.44	0.01	0.28
22.67	−9.37	0.12	0.06	0.18	0.02	0.03				7.22	0.05	0.31
22.33	−9.03	0.23	0.06	0.22	0.03	0.05				5.96	0.04	0.28
22.00	−9.01	0.11	0.06	0.16	0.03	0.02				3.75	0.05	0.24
21.75	−8.71	0.18	0.06	0.25	0.02	0.03				4.51	0.07	0.26
21.50	−9.06	0.25	0.07	0.29	0.02	0.05				4.18	0.08	0.27
21.25	−8.96	0.15	0.06	0.15	0.01	0.04				2.81	0.03	0.24
21.00	−8.92	0.07	0.06	0.13	0.01	0.04				2.69	0.03	0.25
20.75	−8.88	0.21	0.06	0.23	0.02	0.05				7.51	0.07	0.27
20.50	−8.98	0.08	0.05	0.13	0.02	0.03				6.43	0.04	0.26
20.25	−9.39	0.07	0.06	0.13	0.02	0.02				1.51	0.04	0.24
20.00	−9.71	0.28	0.07	0.30	0.02	0.05				7.10	0.09	0.26
19.50	−9.59	0.29	0.07	0.48	0.03	0.07				8.63	0.15	0.31
19.00	−9.53	0.29	0.08	0.49	0.03	0.13	0.24	1.58	0.89	9.23	0.14	0.34
18.67	−9.28	0.08	0.06	0.11	0.02	0.02	0.06	3.03	0.19	1.61	0.02	0.28
18.33	−9.38	0.15	0.06	0.22	0.02	0.04	0.08	2.78	0.52	3.59	0.07	0.31
18.00	−9.28	0.12	0.05	0.19	0.02	0.03	0.07	3.14	0.44	2.37	0.05	0.32
17.67	−9.35	0.16	0.06	0.24	0.02	0.04	0.08	2.63	0.48	3.49	0.08	0.29
17.33	−9.23	0.12	0.05	0.20	0.02	0.05	0.09	1.98	0.43	3.24	0.06	0.31
17.00	−9.37	0.15	0.06	0.26	0.03	0.05	0.22	1.67	6.16	7.51	0.09	0.35
16.50	−9.45	0.21	0.06	0.35	0.04	0.07	0.20	1.49	0.81	5.09	0.12	0.39
16.00	−9.18	0.43	0.08	0.61	0.04	0.08	0.17	0.73	0.98	9.11	0.17	0.38
15.00	−9.03	0.30	0.07	0.46	0.04	0.07	0.16	3.30	0.92	6.38	0.15	0.36
14.00	−9.07	0.32	0.07	0.29	0.03	0.05	0.11	1.69	0.79	8.73	0.09	0.37
13.67	−9.08	0.15	0.05	0.07	0.02	0.02	0.06	1.70	0.50	4.64	0.02	0.31
13.33	−9.25	0.16	0.05	0.09	0.03	0.02	0.07	3.05	0.47	7.51	0.02	0.31
13.00	−9.03	0.04	0.04	0.04	0.02	0.01	0.10	2.35	0.25	1.38	0.01	0.27
12.50	−9.71	0.07	0.04	0.11	0.03	0.02	0.12	1.71	0.28	3.63	0.03	0.31
12.00	−9.51	0.10	0.05	0.17	0.03	0.05	0.08	1.71	0.38	3.55	0.05	0.31
11.50	−9.05	0.09	0.05	0.15	0.03	0.03	0.06	2.33	0.35	3.46	0.05	0.29
11.00	−9.10	0.17	0.06	0.19	0.02	0.04	0.10	1.78	0.44	3.49	0.06	0.23
10.67	−9.06	0.06	0.05	0.12	0.02	0.02	0.07	1.61	0.25	0.78	0.04	0.28
10.33	−8.18	0.16	0.06	0.27	0.02	0.04	0.10	2.14	0.41	2.36	0.08	0.28
10.00	−7.97	0.20	0.07	0.39	0.03	0.05	0.13	3.03	0.54	1.61	0.13	0.30
9.50	−7.42	0.05	0.05	0.12	0.01	0.02	0.05	1.33	0.24	1.57	0.04	0.27
9.00	−7.63	0.13	0.07	0.34	0.01	0.04	0.12	1.50	0.47	2.01	0.07	0.25
8.67	−8.80	0.07	0.06	0.15	0.01	0.02	0.06	1.64	0.35	1.03	0.05	0.30
8.33	−9.48	0.01	0.06	0.06	0.00	0.01	0.08	1.91	0.38	0.29	0.01	0.23
8.00	−9.81	0.02	0.05	0.08	0.01	0.01	0.04	2.68	0.24	0.70	0.02	0.16
7.50	−9.70	0.09	0.06	0.20	0.03	0.06	0.08	1.68	0.36	1.84	0.06	0.32
7.00	−9.65	0.10	0.06	0.19	0.03	0.04	0.08	2.82	0.38	1.63	0.06	0.39
6.50	−9.36	0.27	0.07	0.44	0.03	0.07	0.14	2.27	0.72	3.30	0.13	0.36
6.00	−8.88	0.19	0.06	0.29	0.03	0.05	0.18	1.51	0.62	3.70	0.08	0.32
5.67	−8.32	0.08	0.06	0.09	0.02	0.02	0.08	1.98	0.57	4.00	0.03	0.28
5.33	−7.76	0.11	0.06	0.06	0.01	0.02	0.03	2.61	0.59	4.53	0.02	0.29
5.00	−7.74	0.16	0.06	0.29	0.01	0.03	0.02	4.68	0.68	5.76	0.03	0.29
4.75	−7.39	0.14	0.06	0.54	0.02	0.19	0.15	0.67	1.12	11.25	0.08	0.24
4.50	−7.14	0.02	0.05	0.03	0.01	0.01	0.04	1.60	0.26	2.29	0.01	0.27
4.25	−7.23	0.02	0.05	0.03	0.01	0.01	0.02	1.34	0.25	1.38	0.00	0.25
4.00	−7.28	0.06	0.05	0.06	0.01	0.02	0.05	2.32	0.47	3.56	0.01	0.27
3.67	−7.47	0.38	0.07	1.32	0.02	0.08	0.18	3.54	0.86	6.05	0.11	0.30
3.33	−7.75	0.20	0.09	0.77	0.01	0.08	0.23	3.14	0.67	4.66	0.10	0.35
3.00	−8.05	0.02	0.07	0.04	0.01	0.01	0.02	1.80	0.18	1.37	0.00	0.37
2.50	−8.76	0.12	0.07	0.26	0.02	0.09	0.10	2.37	0.51	1.86	0.07	0.50
2.00	−9.00	0.21	0.08	0.74	0.03	0.13	0.24	3.32	0.61	2.83	0.21	0.48
1.80	−9.18	0.64	0.14	1.95	0.04	0.41	0.50	4.71	1.70	8.96	2.33	0.64
1.60	−9.05	0.24	0.07	0.64	0.03	0.07	0.15	1.32	0.55	2.10	0.15	0.32
1.40	−8.63	0.31	0.08	1.27	0.02	0.21	0.23	3.50	1.09	3.83	0.15	0.54
1.20	−8.12	0.07	0.06	0.22	0.01	0.05	0.08	2.50	0.18	0.80	0.05	0.35
1.00	−8.18	0.03	0.05	0.28	0.01	0.03	0.05	2.48	0.25	1.01	0.02	0.81
0.75	−8.37	0.30	0.11	1.28	0.02	0.55	0.58	4.34	0.97	7.12	0.37	1.57
0.50	−8.59	0.14	0.06	0.65	0.03	0.15	0.19	3.09	0.52	2.49	0.08	1.97
0.25	−7.84	0.14	0.09	0.27	0.03	0.03	0.09	1.05	0.55	2.40	0.15	1.54
0.00	−7.98	0.25	0.13	0.49	0.03	0.05	0.16	0.14	0.88	3.99	0.29	1.50

plateau over the youngest part of the section at ca. 1.5 ppm (Fig. 4f). The increase in U concentration coincides with a significant decrease in $\delta^{234}U_{initial}$ values, in the case of the MC-ICP-MS measurements. $\delta^{234}U_{initial}$ values were calculated using corrected ages, although precise age determinations using these data were unsuccessful because of the above mentioned high detrital content of the stalagmite section.

4.4. Micro-XRF and micro-XANES results

A vertical scan was performed with 100 μm steps proximal (ca. 200 μm) to the uppermost portion of the stalagmite sample. An enhanced U (and Pb) bearing microscopic grain was detected at ca. 1 mm from the end of the sample. A detailed map was made for this part of the stalagmite with an area of $2 \times 1\ mm^2$ using 30 μm horizontal and 20 μm vertical steps. The mapping revealed a belt with minerals rich in U, Th, REE and Pb (see Supplementary material for details). The belt is approximately 1040 μm from the upper margin of the sample and ca. 400 μm thick. Micro-XANES measurements were performed on grains containing U at the highest concentrations and also on the matrix. The interpreted results in comparison with the standards spectra shows that U is in the tetravalent state (same absorption edge as UO_2) within the grains and mostly in the hexavalent state (similar absorption edge as UO_3) in the matrix. However, the relatively low U concentration, and significant amount of Rb and Sr in the sample studied made the XANES measurements problematic in the case of the matrix U.

4.5. Trace elements in trees

Dendrochemical data is characterized by less variability at the early and recent ends of the record and shows some larger peaks in the 1960–1980 period (Fig. 5). To help the interpretation of the dendrochemical record and its potential link to past mining activity the natural range of variability was estimated as double the standard deviation range around the mean for the 1929–1950 pre-mining period. Uranium was an exception again as in the given period the tree rings usually had no detectable U. Only the physiological peak at H/S transition (Thiry et al., 2005) of Kov09 showed measurable U so the natural U concentration in tree rings was regarded as zero.

5. Discussion

5.1. Origin of the U peak

Biologically speaking, U is a non-essential element. It is chemotoxic, radiotoxic and carcinogenic. As U is radioactive, its effects on human health have been widely investigated. In the Earth's crust, the average U content is 2.7 ppm, wheras the average U content in speleothems from most caves is 0.01–2 ppm (Quinif, 1987; Railsback et al., 2002). However, in special cases, as much as 350 ppm U has been reported from aragonitic speleothems (Ortega et al., 2005), due to preferred uranyl incorporation in the aragonite structure (Speer, 1990). In the case of the Trio Cave no aragonitic layers have been observed, therefore, the profound changes in the chemical composition of the stalagmite in the sub-recent section imply variations in dripwater chemistry. With an increased flux of washed-in particles, the U concentration increases greatly in the youngest 1.3 mm of the stalagmite, suggesting mechanisms other than biogenic activity. This is also supported by the uncorrelated high U values in the soil-related variables (P and $\delta^{13}C$). According to the average growth rate of the stalagmite this period represents the latest 30–50 a, which is likely influenced by anthropogenic factors.

Possible anthropogenic sources of U (Reimann and Caritat, 1998) are: (1) phosphate fertilisers, (2) industrial pollution (i.e. ash from coal-fired power plants) and (3) U mining, known to have occurred in the vicinity.

In northern Poland, and also in Croatia and Hungary, anomalously high U concentrations, in surficial water bodies are possibly derived from fertilisers that were produced from phosphorites rich in U (Makweba and Holm, 1993; Kratz and Schnug, 2005). Phosphate-fertilizers may contain considerable amounts of U, ranging from less than 10 to more than 360 mg/kg (Hamato et al., 1995; Salminen, 2005). There is little agricultural activity in the region surrounding the study area which rules out the possibility to U being derived from fertilisers and this is consistent with the absence of high P concentration in the topmost section of the speleothem.

It is also unlikely that coal-derived pollutants carry appreciable U into the cave system. The only potential industrial source of U is in the southern part of Hungary, near Pécs, 12 km SE of the cave site. This source is in the opposite direction to the dominantly westerly winds across the study site. If coal ash were a primary source of U then one would also expect to find increased concentrations of associated metals such as Co, Ni, Zn and V, and this is not observed in the stalagmite. Metal ion (i.e. Ni, Co, Cu, Pb) concentrations are not commonly reported for stalagmites, presumably because of their relatively low concentrations. Piketh et al. (1999) reported an average Cu concentration of 16.2 (±6.1%) ppm. Ortega et al. (2005) found less than the detection limit for Ni and Cu for most of their calcite samples and 4 ± 1 ppm for Ni, and 3 ± 1 ppm for Cu only in two cases. Borsato et al. (2007) measured 1.85–4.73 ppm Cu in their ER78 stalagmite. Black or brown layers of recent laminae of stalagmites in caves open for the public are frequently characterized by elevated Cu and Ti content due to the presence of non-carbonaceous air pollution (Yeong et al., 2003). In the case of the Trio stalagmite black coloured laminae and elevated Co, Zn, Cu or Ni concentrations are not observed (Fig. 4e). The power plant near Pécs was coal-fired until 2003–2004, which implies that pollutants derived from the plant should affect the youngest, recent part of the stalagmite (date of collection: 2001). However, a decrease in U concentration was observed (Fig. 6a) in the youngest portion of the stalagmite record.

A third source of U is from U mines in the area that have been worked over the past four decades. The U ore body lies within a >1000 m thick Permian sandstone. Mining in the area produced 20,000 t of U concentrate during its operation, extracted from millions of tons of worked ore (Bánik et al., 2002). Industrial scale production started around 1959, and was further developed between 1965 and 1975 (Fig. 2). Ore production was completed in 1997 and The maximum U load on the environment lasted for ca. 20 a, from 1970 to 1990 (Fig. 2).

The catchment area of the Trio Cave is situated above the elevation of the closest mine-pits (Nos. IV and V), so U could not have followed a fluvial course to the cave. Eolian transport is much more likely. The U mine was ventilated by air shafts, and the mass of sandstone mined for U is directly correlated with the dust released through ventilation shafts. Eolian transport of dust released from air shafts and subsequent deposition have been identified by previous studies of soils, plants and leaves (Mecsekérc Ltd., unpublished reports). Elevated ^{210}Pb activities were detected in leaf material collected near ventilation shafts and along wind trajectories of anticipated fallout.

Elemental data provide further constraints on the source of U. Elevated concentrations of Si, Al and Th within the stalagmite are associated with detrital sources (White, 1997). A hiatus caused by drier periods could be responsible for elevated concentrations of Si, Al and Th, but these hiatuses may have been short-lived, as

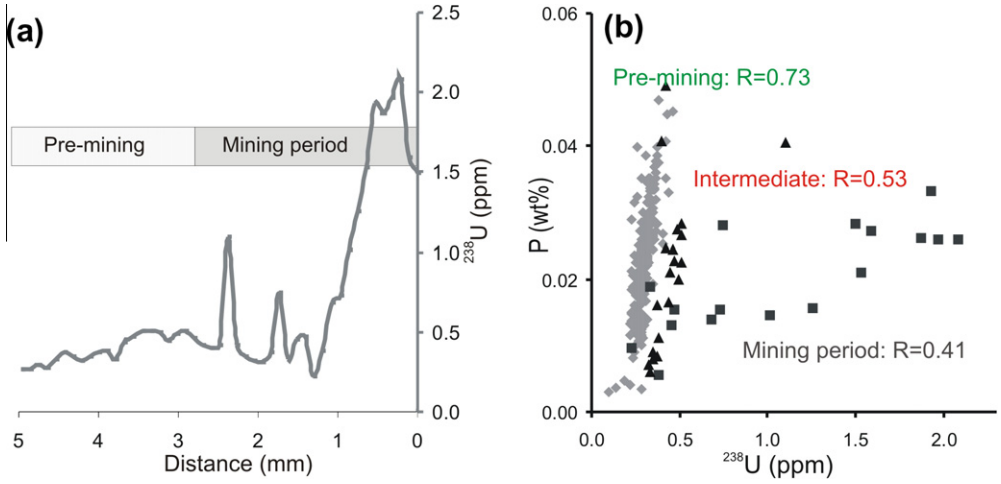

Fig. 6. ^{238}U concentration for the topmost 5 mm of the stalagmite and the assumed period of mining activity. Note that concentration is decreasing at the very top of the stalagmite. Correlation between P and U for assumed pre-mining and mining period of the studied sample. Intermediate period is also indicated. Note the reduction of the R^2-values and the change in the P/U ratio.

no single detritus-layers were detected within the stalagmite's microstructure based on optical microscopic observations. The cyclical variation of the chemical record (i.e. δ^{13}C and P data) without abrupt peaks and troughs is consistent with a lack of distinct hiatuses. Evenly distributed detrital material is observed within the stalagmites, with distinct cycles of the above mentioned elements. This could be caused by variable growth rate, resulting in relative enrichment of impurities and increased surficial weathering or in enhanced infiltration of detrital impurities. In this case elements other than Si, Al and Th should also have higher concentrations within the $CaCO_3$ matrix, but they were not enriched in this particular section of the stalagmite.

The results of the LA-ICP-MS scan along a 27 mm section are plotted in Fig. 4b. Notable peaks of Si and Al (at 4.53, 2.48, 1.51 and 0.54 mm) and Th (at 2.38–2.27 mm) were observed to be superimposed on the elevated background for the elements. A change in the amount of precipitation was not detected at two meteorological stations in the vicinity of the site (ca. 4 and 12 km away; see Supplementary material for details), which implies that impurities do not result from shifts in infiltration or weathering.

Although the higher proportion of washed-in particles can be clearly followed by the elevated detrital content of the stalagmite, exceptionally high Si, Al and Th peaks are observed to coincide with the optically darker and chemically U-enriched layers (Fig. 4a and b). The gradual increase in U concentration to the highest values (0.2–2.1 ppm), therefore, may be due to the weathering and/or transport of the mine-derived dust that settled in the catchment area.

Variability in the concentration of P can be attributed to paleovegetation and/or paleohydrology changes (Huang et al., 2001; Treble et al., 2003). Plotting P vs. U is used here to distinguish between the assumed pre-mining period and active mining period, as they are characterized by different elemental ratios (Fig. 6b). The earlier portion of the stalagmite is characterized by systematic co-variation of U and P with low concentrations for both elements. This pattern implies that these elements responded rapidly to vegetation changes. Higher P concentrations coincide with lower δ^{13}C values reflecting increases in vegetation and soil biological activity, as C-isotopes are controlled to some extent by soil activity (Dorale et al., 1992; Johnson et al., 2006). Changes in the δ^{13}C values of stalagmites can be caused by a number of different factors, including: changes in the relative contributions of soils and aquifer limestone to the dissolved inorganic C (Genty et al., 1998) vegetation type (C3–C4; Dulinski and Rozanski, 1990; McDermott, 2004 and references therein), and fluid pathways, degassing and prior calcite precipitation from supersaturated water (Baker et al., 1997; Spötl et al., 2005; Johnson et al., 2006). Secondary processes, however (i.e. kinetic fractionation during the deposition of the carbonate; Mickler et al., 2004) may obscure the primary C-isotopic signal. Kinetic effects would lead to simultaneous enrichment of ^{13}C isotopes in the calcite (Hendy, 1971). In the case of the Trio stalagmite, a moderate negative correlation was observed between δ^{13}C and P (r-value < −0.5). Soil and drip water is expected to carry more negative δ^{13}C values and increased P concentrations during active vegetation periods. Thus it may be may assumed that variations in P concentration and δ^{13}C values are primarily influenced by soil (vegetation) activity, not kinetic effects.

The anomalously high concentration of U during the deposition of the sub-recent section of the stalagmite requires additional consideration. In order to determine the differences in the U sources, δ^{234}U values were determined for the older part of the stalagmite and for the sub-recent part. ^{234}U/^{238}U ratios have been used as a proxy for paleoprecipitation at much longer time scales (i.e. tens of ka, Kaufman et al., 1998; Zhou et al., 2005). The Trio stalagmite, however shows a notable δ^{234}U value decrease within a short period, with elevated detrital element contents and U concentrations, suggesting changes in the source of U, i.e. an external flux of U-bearing material into the catchment area of the Trio Cave. Thus, the rapid increase in U concentration of the speleothem and a smaller decrease just below the recent surface are controlled by weathering and infiltration of the fall-out material. The LA-ICP-MS technique did not provide information on the microscopic heterogeneity and the chemical form of U present in the stalagmite sample. The synchrotron based X-ray analytical methods (micro-XRF and XANES) used revealed that U measured by LA-ICP-MS is present not only in the hexavalent state, substituting for Ca in the stalagmite matrix but also in the tetravalent state related to accessory minerals (see Supplementary material for details). Thus higher U concentrations in the hexavalent state represent dissolved and co-precipitated U-phases, from an oxidizing environment. Accessory U-bearing minerals migrating through the soil and karst system as insoluble particles had a tetravalent state. The present investigation finds that within the section showing the U-anomaly the U-bearing minerals are present in a distinct zone, which may represent a period with abundant washed-in particles into the karst system.

5.2. Timing of the pollution

Age determination of the beginning of pollution, transportation and mobility of U in the karstic environment is not feasible due to the lack of precise age control over the recent part, as discussed above. Using dendrochemical data from the pine trees enables confirmation of the existence of pollution and inferring of time leads and lags between the mine-pit openings and the migration of the pollution within the studied area, and so can further infer the age of the sub-recent part of the stalagmite that contains the U anomaly.

Anomalies in the trace element record (Fig. 5) broadly correspond with the period of nearby mining activity. A detailed comparison between the major shifts in the dendrochemical record and the opening dates and exploitation peaks provide additional information.

Focusing on U, the main interest of the present study, the first peak at 1946 in Kov09 comes from near the H/S transition. The second U peak is dated to the late 1950s and is accompanied by a distinct Cu peak co-occuring in Kov06 and Kov09. In the case of Kov06 it corresponds to the H/S transition however Kov09 also contains relatively elevated U values from 1956 to 1957 that cannot be explained by physiological processes linked to H/S transition. This date closely follows the initiation of the mining activity of the region as Pit II opened in 1954. The other U-peaks found in younger tree rings also cannot be interpreted by physiological processes and suggest an episodically enhanced U accumulation.

Trace metals show abrupt increases in the tree rings dated to 1965. This date fits perfectly to the opening of the Shaft IV and each studied element shows elevated values in tree rings dated to the late 1960s. Manganese and Zn maintain anomalously high levels until ~1980. Mine openings require industrial scale welding equipment and operations for pipe and tube connections. Alloy electrode wires for welding in a controlled CO_2 atmosphere contains Mn (and Si) as a contributor for expelling (Mn) oxide from the surface of the alloy or removing the oxide film from the base metal, in order to reduce the formation of inclusions (HSDB, 1999). Manganese is a major component of welding fumes (Bowler et al., 2007); therefore, it is assumed that an increased demand on metal welding during the mine shaft openings may have caused elevated Mn emission overlapping certain years. Manganese could be transported into the karst system mainly as organic complexes (Richter et al., 2004), colloidal hydroxides and/or particles by the infiltrating water. Most of the elements (Cu is an exception) reach their highest levels within this section over the studied period. The dendrochronologically derived date of tree rings characterized by elevated metal levels matches the most intense mining period. The highest values of U relative intensities are mismatched in the pine trees however, and lie near each other; i.e. 1968 in Kov09 and 1971 in Kov 06.

The last exploitation phase was launched in 1991 and spanned 4 years. This is mirrored in the Cu and U record. However Mn and Zn do exceed the range of natural variability during this period. The rest of the recent section of the dendrochemical record has no anomalously high values for the studied chemical species.

Due to the observed coincidences between the major changes in the dendrochemical record and the most characteristic events of the U-mining history causality is highly presumable. This implies that the pine trees preserved particles that were emitted from the nearby U-mines and these particles reached and affected the surface environment at the divide, and probably affected an even larger part of the watershed of the Trio Cave.

The most prominent features of the Trio Cave stalagmite record are the rapid increases in U concentration by an order of magnitude, decreases in $\delta^{234}U$ values and well-marked oscillations of detrital elements (Al, Si, Th) at the topmost ca. 2 mm of the stalagmite. The source of the drip water from which these chemical compounds originated is the catchment of the cave. The thickness of karstic rocks above the speleothem is ca. 15 m and the irregular field observations suggest a short lag time between surface precipitation events and increasing drip intensity at the stalagmite. Therefore, it is reasoned that no significant time shift exists between the date of surface pollution and the pollutant deposition into the speleothem. It is also expected that only slight mixing and dilution of the seepage water can occur in the vadose zone. This can explain the smoothed signal for water soluble U and the lack of separate U peaks related to individual mine-pit openings. The 1970s can be assigned as the most likely date for the largest U-peak in the speleothem record. Considering that pine trees record major pollution of the water shed after 1965, a peak around 1970, and assuming some time lag due to the seepage through the epikarst.

6. Conclusions

The present study presents a sedimentary and biological record (recent stalagmite and pine tree) of two different geochemical proxies as pollution recorders. The stalagmite displays a clear U anomaly in the second half of the 20th century, however, the precise timing of its record is uncertain. The relationship between major changes in the U content and $\delta^{234}U$ values of the speleothem, the coincidences between the non-physiological changes in the dendrochemical record and the history of U ore production strongly suggest a causal link. The study demonstrates that the Scots pine specimen preserved particles emitted from the nearby U-mines and these particles reached and affected the catchment area of the Trio Cave. The importance of these proxies is highlighted as an important record of environmental contamination in the past, when detailed emission information and possible deposition rates from pollutant sites are not available. The results show that stalagmites can record environmental impacts, and thus reliably preserve environmental pollution signals, a hitherto largely unexplored source of information that can help in environmental monitoring. The mobility of U in a karstic system through the soil zone was studied indirectly, and higher incorporation of U into the matrix of the stalagmite and higher concentration of U-bearing minerals, as detrital particles, was shown.

Acknowledgements

We thank G.S. Burr, University of Arizona, for constructive suggestions. This study was financially supported by the Hungarian Scientific Research Fund (OTKA T 049713 and K 67583) and TÁMOP 4.2.1./B-09/KMR-2010-0003. Measurements of U–Th isotopic compositions and ^{230}Th dates were supported by the National Science Council Grants (97-2752-M002-004-PAE, 99-2628-M002-012, 99-2611-M002-005 to C.-C.S.) and the Hungarian Academy of Sciences (travel grants to Z.S.). This paper is a contribution to the Millennium Project (No. 017008). XANES measurements received funding from the European Community's FP7 (No. 226716).

Appendix A. Supplementary material

Supplementary data associated with this article can be found, in the online version, at doi:10.1016/j.apgeochem.2011.01.025.

References

Baillie, M.G.L., 1995. Dendrochronology and Precision Dating, B.T. A Slice Through Time. Batsford Ltd., London.

Baker, A., Ito, E., Smart, P.L., McEwan, R.F., 1997. Elevated and variable values of ^{13}C in speleothems in a British cave system. Chem. Geol. 136, 263–270.

Baker, A., Smart, P.L., Barnes, W.L., Edwards, R.L., Farrant, A.R., 1995. The Hekla 3 volcanic eruption recoded in a Scottish speleothem? Holocene 5, 336–342.
Bánik, J., Csicsák, J., Berta, Zs., 2002. Experience on application of continuous drain trench during the remediation of tailings ponds in Hungary. In: Merkel, B.J., Planer-Friedrich, P.-F., Wolkersdorfer, C. (Eds.), Uranium Mining and Hydrogeology III, pp. 913–921.
Barabás, A., Barabás-Stuhl, Á., 2005. Geology of the Lower Triassic Jakabhegy Sandstone Formation, Hungary, SE Transdanubia. Acta Geol. Hung. 48, 1–47.
Barrelet, T., Ulrich, A., Rennenberg, H., Krähenbühl, U., 2006. Seasonal profiles of sulphur, phosphorus and potassium in Norway spruce wood. Plant Biol. 8, 462–469.
Bellis, D., Ma, R., Bramall, N., McLeod, C.W., Chapman, N., Satake, K., 2001. Airborne uranium contamination – as revealed through elemental and isotopic analysis of tree bark. Environ. Pollut. 114, 383–387.
Bleahu, M., Mantea, G., Bordea, S., Panin, S., Stefanescu, M., Sikic, K., Haas, J., Kovács, S., Péró, Cs., Bérczi-Makk, A., Konrád, Gy., Nagy, E., Rálisch-Felgenhauer, E., Török, Á., 1996. Triassic facies types, evolution and paleogeographic relations of the Tisza Megaunit. Acta Geol. Hung. 37, 187–234.
Borsato, A., Frisia, S., Fairchild, I.J., Somogyi, A., Susini, J., 2007. Trace element distribution in annual stalagmite laminae mapped by micrometer-resolution X-ray fluorescence: Implications for incorporation of environmentally significant species. Geochim. Cosmochim. Acta 71, 1494–1512.
Bowler, R.M., Roels, H.A., Nakagawa, S., Drezgic, M., Park, R., Koller, W., Bowler, R.P., Mergler, D., Bouchard, M., Smith, D., Gwiazda, R., Doty, R.L., 2007. Dose-effect relationships between manganese exposure and neurological, neuropsychological and pulmonary function in confined space bridge welders. Occup. Environ Med. 64, 167–177.
Bozsó, Z., 1999. A study of One Environmental Problem Related to the U-ore Mining in the Mecsek-mts. University of Szeged, MSc Thesis. (in Hungarian).
Cooksey, C., Hyland, J., 2007. Sediment quality of the Lower St. Johns River, Florida: an integrative assessment of benthic fauna, sediment-associated stressors, and general habitat characteristics. Marine Pollut. Bull. 54, 9–21.
Costagliola, P., Benvenuti, M., Chiarantini, L., Bianchi, S., Benedetto, F.D., Paolieri, M., Rossato, L., 2008. Impact of ancient metal smelting on arsenic pollution in the Pecora River Valley, Southern Tuscany, Italy. Appl. Geochem. 23, 1241–1259.
Cutter, B.E., Guyette, R.P., 1993. Anatomical, chemical and ecological factors affecting tree species choice in dendrochemistry studies. J. Environ. Qual. 22, 611–619.
Dorale, J.A., Gonzalez, L.A., Reagan, M.K., Pickett, D.A., Murrell, M.T., Baker, R.G., 1992. A high-resolution record of Holocene climate change in speleothem calcite from Cold Water Cave, Northeast Iowa. Science 258, 1626–1630.
Dulinski, M., Rozanski, K., 1990. Formation of $^{13}C/^{12}C$ isotope ratios in speleothems: a semi-dynamic model. Radiocarbon 32, 7–16.
Dunca, E., Schöne, B.R., Mutvei, H., 2005. Freshwater bivalves tell of past climates: but how clearly do shells from polluted rivers speak? Palaeogeog. Palaeoclim. Palaeoecol. 228, 43–57.
Elless, M.P., Lee, S.Y., 1998. Uranium solubility of carbonate-rich uranium-contaminated soils. Water Air Soil Pollut. 107, 147–162.
Fairchild, I.J., Loader, N.J., Wynn, P.M., Frisia, S., Thomas, P.S., Lageard, J.G.A., de Momi, A., Hartland, A., Borsato, A., La Porta, N., Susini, J., 2009. Sulfur fixation in wood mapped by synchrotron X-ray studies: implications for environmental archives. Environ. Sci. Technol. 43, 1310–1315.
Fairchild, I.J., Smith, C.L., Baker, A., Fuller, L., Spötl, C., Mattey, D., McDermott, F.E.I.M.F., 2006. Modification and preservation of environmental signals in speleothems. Earth Sci. Rev. 75, 105–153.
Fazekas, V., 1987. Mineralogy of the permian and lower triassic sandstone formations. Földtani Közlöny 117, 11–30. in Hungarian.
Ferretti, M., Innes, J.L., Jalkanen, R., Saurer, M., Schaffer, J., Spiecker, H., von Wilpert, K., 2002. Air pollution and environmental chemistry – what role for tree-ring studies? Dendrochronologia 20, 159–174.
Finch, R., Murakami, T., 1999. Systematics and paragenesis of uranium minerals. In: Burns, P.C., Finch R. (Eds.), Uranium: Mineralogy, Geochemistry and the Environment. Reviews in Mineralogy, pp. 91–180.
Frisia, S., Borsato, S., Susini, J., Somogyi, A., 2005. Climate forcings and their influence on Alpine history as reconstructed through the application of synchrotron-based X-ray microfluorescence on layered stalagmites. Archaeometry 47, 209–219.
Fritz, E., 2007. Measurement of cation exchange capacity (CEC) of plant cell walls by X-ray microanalysis (EDX) in the transmission electron microscope. Microsc. Microanal. 13, 233–244.
Frohlich, C., Hornbach, M.J., Taylor, F.W., Shen, C.-C., Moala, A., Morton, A.E., Kruger, J., 2009. Huge erratic boulders in Tonga deposited by a prehistoric tsunami. Geology 37, 131–134.
Gascoyne, M., 1992. Geochemistry of the actinides and their daughters. In: Ivanovich, M., Harmon, R.S. (Eds.), Uranium-Series Disequilibrium: Applications to Earth, second ed., Marine, and Environmental Sciences Clarendon Press, Oxford, pp. 4–61.
Genty, D., Vokal, B., Obelic, B., Massault, M., 1998. Bomb ^{14}C time history recorded in two modern stalagmites – importance for soil organic matter dynamics and bomb ^{14}C distribution over continents. Earth Planet. Sci. Lett. 160, 795–809.
Günther, D., Frischknecht, R., Heinrich, C.A., Kahlert, H.J., 1997. Capabilities of an argon fluoride 193 nm excimer laser for laser ablation inductively coupled plasma mass spectrometry microanalysis of geological materials. J. Anal. Atom. Spectrom. (12/9), 939–944.
Guyette, R.P., Cutter, B.E., Henderson, G.S., 1991. Long-term relationship between mining activity and levels of lead and cadmium in tree-rings of eastern red cedar. J. Environ. Qual. 20, 146–150.
Guyette, R.P., Henderson, G.S., Cutter, B.E., 1992. Reconstructing soil pH from manganese concentration in tree-rings. Forest Sci. 38, 727–737.
Hagemeyer, J., Schäfer, H., 1995. Seasonal variations in concentrations and radial distribution patterns of Cd, Pb and Zn in stem wood of beech trees (*Fagus sylvatica* L.). Sci. Total Environ. 166, 77–87.
Hamato, H., Landsberger, S., Harbottle, G., Panno, S., 1995. Studies of radioactivity and heavy metals in phosphate fertilizer. J. Radioanal. Nucl. Chem. 194, 331–336.
Hantemirov, R.M., 1992. Possibility to use chemical elements in tree rings of Scots pine for the air pollution reconstruction. In: Bartholin, T., Berglund, B.E., Eckstein, D., Schweingruber, F.H. (Eds.), Tree Rings and Environment, LUNDQUA Report 34, pp. 142–145.
Hendy, C.H., 1971. The isotopic geochemistry of speleothems: I. The calculation of the effects of different modes of formation on the isotopic composition of speleothems and their applicability as palaeoclimatic indicators. Geochim. Cosmochim. Acta 35, 801–824.
Hill, C.A., Forti, P., 1997. Cave Minerals of the World. National Speleological Society, Huntsville, Alabama, USA.
Hoffmann, E., Lüdke, C., Scholze, H., Stephanowitz, H., 1994. Analytical investigation of tree rings by laser ablation ICP-MS. Fres. J. Anal. Chem. 350, 253–259.
Holmes, R.L., 1983. Computer-assisted quality control in tree-ring dating and measurements. Tree-Ring Bull. 43, 69–75.
HSDB 1999. Hazardous Substances Data Bank. National Library of Medicine, Bethesda, Maryland. WWW database <http://toxnet.nlm.nih.gov/cgi-bin/sis/search/f?./temp/~yrZuzn:1>.
Huang, Y., Fairchild, I.J., Borsato, A., Frisia, S., Cassidy, N.J., McDermott, F., Hawkesworth, C.J., 2001. Seasonal variations. In: Sr, Mg and P in Modern Speleothems (Grotta di Ernesto, Italy). Chem. Geol. vol. 175, pp. 429–448.
Johnson, K.R., Hu, C., Belshaw, N.S., Henderson, G.M., 2006. Seasonal trace-element and stable isotope variations in a Chinese speleothem: the potential for high resolution paleomonsoon reconstruction. Earth Planet. Sci. Lett. 244, 394–407.
Kaennel M., Schweingruber, F.H., 1995. Multilingual Glossary of Dendrochronology. Paul Haupt, Bern.
Kaufman, A., Wasserburg, G.J., Porcelli, D., Bar-Matthews, M., Ayalon, A., Halicz, L., 1998. U–Th isotope systematics from the Soreq Cave, Israel, and climatic correlations. Earth Planet. Sci. Lett. 156, 141–155.
Kern, Z., Popa, I., Varga, Zs., Széles, É., 2009. Degraded temperature sensitivity of a stone pine chronology explained by dendrochemical evidences. Dendrochronologia 27, 121–128.
Kratz, S., Schnug, E., 2005. Rock phosphates and P fertilizers as sources of U contamination in agricultural soils. In: Merkel, B. J., Hasche-Berger, A. (Eds.), Uranium Mining and Hydrogeology IV, pp. 57–67.
Langmuir, D., 1978. Uranium solution-mineral equilibria at low temperatures with applications to sedimentary ore deposits. Geochim. Cosmochim. Acta 42, 547–569.
Makweba, M.M., Holm, E., 1993. The natural radioactivity of the rock phosphates, phosphatic products and their environmental implications. Sci. Total Environ. 133, 99–110.
McCrea, J.M., 1950. On the isotopic chemistry of carbonates and a paleotemperature scale. J. Chem. Phys. 18, 849–857.
McDermott, F., 2004. Palaeo-climate reconstruction from stable isotope variations in speleothems: a review. Quatern. Sci. Rev. 23, 901–918.
Mickler, P.J., Banner, J.L., Stern, L., Asmerom, Y., Edwards, R.L., Ito, E., 2004. Stable isotope variations in modern tropical speleothems: evaluating equilibrium vs. kinetic isotope effects. Geochim. Cosmochim. Acta 68, 4381.
Monticelli, D., di Iorio, A., Ciceri, E., Castellini, A., Dossi, C., 2009. Tree ring microanalysis by LA–ICP–MS for environmental monitoring: validation or refutation? Two case histories. Microchim. Acta 164, 139–148.
Nagy, E., 1968. Triassic Formation of the Mecsek-mts. (A Mecsek-hegység triász időszaki képződményei – *in Hungarian).* MÁFI Annual Report. 51/1, p. 198.
Ortega, R., Maire, R., Deves, G., Quinif, Y., 2005. High-resolution mapping of uranium and other trace elements in recrystallized aragonite–calcite speleothems from caves in the Pyrenees (France): implication for U-series dating. Earth Planet. Sci. Lett. 237, 911–923.
O'Sullivan, P.E., 1983. Annually-laminated lake sediments and the study of Quaternary environmental changes – A review. Quaternary Sci. Rev. 1/4, 245–313.
Panov, B.S., Dudik, A.M., Shevchenko, O.A., Matlak, E.S., 1999. On pollution of the biosphere in industrial areas: the example of the Donets coal Basin. Internat. J. Coal Geol. 40, 199–210.
Pearson, C., Manning, S.W., Coleman, M., Jarvis, K., 2005. Can tree-ring chemistry reveal absolute dates for past volcanic eruptions? J. Archaeol. Sci. 32, 1265–1274.
Pearson, C., Manning, S.W., Coleman, M., Jarvis, K., 2006. A dendrochemical study of Pinus sylvestris from Siljansfors Experimental Forest, central Sweden. Appl. Geochem. 21, 1681–1691.
Perin, G., Fabris, R., Mabente, S., Rebello, I., Wagener, A., Hamacher, C., Scotto, S., 1997. A Five-year study on the heavy-metal pollution of Guanabara bay sediments (Rio de Janeiro, Brazil) and evaluation of the metal bioavailability by means of geochemical speciation. Water Res. 31, 3017–3028.
Perrette, Y., Poulenard, J., Saber, A-I., Fanget, B., Guittonneau, S., Ghaleb, B., Garaudee, S., 2008. Polycyclic Aromatic Hydrocarbons in stalagmites: occurrence and use for analyzing past environments. Chem. Geol. 251, 67–76.

Piketh, S.J., Sideras-Haddad, E., Holmgren, K., Tyson, P.D., 1999. Proton micro-probe analysis of a speleothem from South Africa. Nucl. Instrum. Methods B 158, 606–611.

Prohaska, T., Stadlbauer, C., Wimmer, R., Stingeder, G., Latkoczy, Ch., Hoffmann, E., Stephanowitz, H., 1998. Investigation of element variability in tree rings of young Norway spruce by laser-ablation-ICPMS. Sci. Total Environ. 219, 29–39.

Quinif, Y., 1987. Concentrations anomales en uranium dans les stalagmites (gouffre de la Pierre Saint-Martin, Pyrénées, France). Bull. Soc. Belge Geol. 96, 121–128.

Railsback, L.B., Dabous, A.A., Osmond, J.K., Fleisher, C.J., 2002. Petrographic and geochemical screening of speleothems for U-series dating: an example from recrystallized speleothems from Wadi Sannur Cavern, Egypt. J Cave Karst Studies (64/2), 108–116.

Reimann, C., de Caritat, P., 1998. Chemical Elements in the Environment – Factsheets for the Geochemist and Environmental Scientist. Springer–Verlag, Berlin, Germany.

Ribera, D., Labrot, F., Tisnerat, G., Narbonne, J.-F., 1996. Uranium in the environment: occurrence, transfer, and biological effects. Rev. Environ. Contam. Toxicol. 146, 56–89.

Richard, D.A., Dorale, J.A., 2003. Uranium-series chronology and environmental applications of speleothem. In: Bourdon, B., Henderson, G.M., Lundstrom, C.C., Turner, S.P. (Eds.), Uranium-series Geochemistry. Reviews in Mineralogy and Geochemistry, vol. 52, pp. 407–460.

Richter, D.K., Götte, T., Niggemann, S., Wurth, G., 2004. REE^{3+} and Mn^{2+} activated cathodoluminescence in lateglacial and Holocene stalagmites of central Europe: evidence for climatic processes? Holocene 14, 759–767.

Rinn, F., 2005. TSAP Reference Manual.

Sachs, S., Geipe, G., Mibus, J., Bernhard, G., 2005. Impact of humic acid on the uranium migration in the environment. In: Merkel, B.J., Hasche-Berger, A. (Eds.), Uranium Mining and Hydrogeology IV, pp. 107–116.

Salminen, R., (Chief – Ed.), 2005. Uranium. (In. Geochemical Atlas of Europe; the Association of the Geological Surveys of The European Union (EuroGeoSurveys)/ the Geological Survey of Finland, pp. 389–394.

Saunders, J.E., Al Zahed, K.M., Paterson, D.M., 2007. The impact of organic pollution on the macrobenthic fauna of Dubai Creek (UAE). Marine Pollut. Bull. 54, 1715–1723.

Schettler, G., Romer, R.L., 2006. Atmospheric Pb-pollution by pre-medieval mining detected in the sediments of the brackish karst lake An Loch Mór, western Ireland. Appl. Geochem. 21, 58–82.

Schulz, H., Popp, P., Huhn, G., Stärk, H.-J., Schüürmann, G., 1999. Biomonitoring of airborne inorganic and organic pollutants by means of pine tree barks. I. Temporal and spatial variations. Sci. Total Environ. 232, 49–58.

Shen, C.-C., Edwards, R.L., Cheng, H., Dorale, J.A., Thomas, R.B., Moran, S.B., Weinstein, S.E., Edmonds, H.N., 2002. Uranium and thorium isotopic and concentration measurements by magnetic sector inductively coupled plasma mass spectrometry. Chem. Geol. 185, 165–178.

Shen, C.-C., Cheng, H., Edwards, R.L., Moran, S.B., Edmonds, H.N., Hoff, J.A., Thomas, R.B., 2003. Measurement of attogram quantities of ^{231}Pa in dissolved and particulate fractions of seawater by isotope dilution thermal ionization mass spectroscopy. Anal. Chem. 75, 1075–1079.

Shen, C.-C., Kano, A., Hori, M., Lin, K., Chiu, T.-C., Burr, G.S., 2010. East Asian monsoon evolution and reconciliation of climate records from Japan and Greenland during the last deglaciation. Quaternary Sci. Rev. 29, 3327–3335.

Sheppard, P.R., Witten, M.L., 2005. Laser trimming tree-ring cores for dendrochemistry of metals. Tree-Ring Res. 61, 87–92.

Siklosy, Z., Demeny, A., Vennemann, T.W., Kramers, J., Lauritzen, S.E., Leel-Ossy, Sz., 2007. Middle bronze age climate change recorded in a Hungarian stalagmite: triggering by volcanic activity? Geophys. Res. Abst. 9 1607-7962/gra/EGU2007-A-00777.

Siklosy, Z., Demény, A., Vennemann, T.W., Pilet, S., Kramers, J., Leél-Ossy, Sz., Bondár, M., Shen, C-C., Hegner, E., 2009. Bronze Age volcanic event recorded in stalagmites by combined isotope and trace element studies. Rapid Commun. Mass Spec. 23, 801–808.

Smith, K.T., Shortle, W., 1996. Tree biology and dendrochemistry. In: Dean, J.S., Meko, D.M., Swetnam, T.W. (Eds.), Tree Rings, Environment and Humanity. Radiocarbon, Tucson, AZ, pp. 629–635.

Speer, J.A., 1990. Crystal chemistry and phase relations of orthorhombic carbonates. In: Reeder, R.J. (Ed.), Carbonates: Mineralogy and Chemistry, vol. 11. Mineralogy Society of America, Washington, DC, pp. 145–190.

Spötl, C., Vennemann, T.W., 2003. Continuous-flow IRMS analysis of carbonate minerals: Rapid Comm. Mass Spectrom. 17, 1004–1006.

Spötl, C., Fairchild, I.J., Tooth, A.F., 2005. Cave air control on dripwater geochemistry, Obir Caves (Austria): implications for speleothem deposition in dynamically ventilated caves. Geochim. Cosmochim. Acta 69, 2451–2468.

Spötl, C., Mangini, A., Frank, N., Eichstädter, R., Burns, S.J., 2002. Start of the last interglacial period at 135 ka: evidence from a high Alpine speleothem. Geology 30, 815–818.

Stokes, M.A., Smiley, T.L., 1968. An Introduction to Tree-Ring Dating. The University of Chigago Press, Chicago, IL.

Thiry, Y., Schmidt, P., Van Hees, M., Wannijn, J., Van Bree, P., Rufyikiri, G., Vandenhove, H., 2005. Uranium distribution and cycling in Scots pine (Pinus sylvestris L.) growing on a revegetated U-mining heap. J. Environ. Radioact. 81, 201–219.

Treble, P., Shelley, J.M.G., Chappell, J., 2003. Comparison of high resolution sub-annual records of trace elements in a modern (1911-1992) speleothem with instrumental climate data from southwest Australia. Earth Planet. Sci. Lett. 216, 141–153.

Wang, X.F., Auler, A.S., Edwards, R.L., Cheng, H., Ito, E., Solheid, M., 2006. Interhemispheric anti-phasing of rainfall during the last glacial period. Quaternary Sci. Rev. 25, 3391–3403.

Watmough, S.A., 1999. Monitoring historical changes in soil and atmospheric trace metal levels by dendrochemical analysis. Environ. Pollut. 106, 391–403.

White, W.B., 1997. Color of speleothems. In: Hill C.A., Forti P. (Eds.), Cave Minerals of the World. National Speleological Society: 1-879961-07-5.

Whitlock, C., Dean, W., Rosenbaum, J., Stevens, L., Fritz, S., Bracht, B., Power, M., 2008. A 2650-year-long record of environmental change from northern Yellowstone National Park based on a comparison of multiple proxy data. Quatern. Internat. 188, 126–138.

Yeong, G.Y., Kim, S.J., Chang, S.J., 2003. Black carbon pollution of speleothems by fine urban aerosols in turist caves. Am. Mineral. 88, 1872–1878.

Zhou, J., Lundstrom, C.C., Fouke, B., Panno, S., Hackley, K., Curry, B., 2005. Geochemistry of speleothem records from southern Illinois: Development of $(^{234}U)/(^{238}U)$ as a proxy for paleoprecipitation. Chem. Geol. 221, 1–20.